Int. J. Electrochem. Sci., 2 (**2007**) 72 - 81

International Journal of ELECTROCHEMICAL SCIENCE
www.electrochemsci.org

Influence of Metal Salt Ratio on Ni-Fe-P Film by Chemical Process

Gui-Fang Huang[*], *Jian-Qin Deng, Wei-Qing Huang, Ling-Ling Wang, Bing-Suo Zou, Liang Dong*

College of Physics and microelectronics Science, Hunan University, Changsha 410082, China
[*]Email: huanggfhao@yahoo.com

Received: 25 October 2006 / *Accepted:* 7 December 2006 / *Published:* 1 January 2007

In this paper, the influence of metal salt ratio on the plating rate, composition, and structure of Ni-Fe-P films deposited by chemical process from sulphate bath was investigated. Gravimetric and electrochemical measurements, SEM, XRD were applied to characterize the films. The weight of Ni-Fe-P film increases near linearly with the plating time. The deposition potential shifts to negative direction and the plating current decreases with the increase of $FeSO_4$, when the total concentration of the metal salts is fixed in bath. Increasing the $FeSO_4$ concentration also causes an increase in the polarization resistances, indicating the $FeSO_4$ has an inhibition effect on the chemical process. The plating current derived in the complete bath is higher than that determined from the simulation half-reaction cells due to the interaction between the two half reactions. It is found that the ratio of $FeSO_4/(NiSO_4+FeSO_4)$ affects the composition of Ni-Fe-P film, leading to the structure change of the film.

Keywords: Chemical process, Ni-Fe-P, Polarization, Metal salt

1. INTRODUCTION

Known for their excellent magnetic properties, Fe-Ni alloys are studied extensively and applied widely in various fields[1-12].The addition of a small amount of P or B improves the synthetic magnetic properties of permalloy films by increasing the resistivity value (ρ) [13–15]. Moreover, the presence of P or B in Fe-Ni film can control the iron content via Fe-P or Fe-B codeposition and bring about an amorphous structure, which improves the ductility, corrosion resistance properties[16,17].

There are a variety of thin film formation techniques. Sputtering and evaporation are among the dry process techniques, while electroplating and chemical deposition constitute the wet process. The advantage of the wet process is high productivity. In particular, chemical deposition process is an autocatalytic process with the metal as a final product due to the chemical reduction of the metal cations through reductants in the bath and can be used to produce uniformly thick, hard and corrosion-

resistant films on various material substrates with different shapes[7,15-27]. Thus, it is one of the most important techniques for uniform film formation. Chemical deposition Ni–Fe–P films were first obtained by Wang et al.[18] and followed by other group. These studies reported the effect of bath components and plating conditions on the plating rate, composition, structure and microhardness of Ni-Fe-P films[7,18,22]. However, there are little reports on the electrochemical characteristic of Ni–Fe–P deposition process.

In this paper, we investigate the effects of ratios of $FeSO_4/(NiSO_4+FeSO_4)$ in the bath on the Ni-Fe-P films from alkaline solutions. XRD, SEM, gravimetric and electrochemical measurements were employed to characterize the Ni-Fe-P films.

2. EXPERIMENTS

A basic hypophosphite reduced sulphate bath was chosen as the plating bath, where nickel sulphate and iron sulphate were used as the source of metal while sodium hypophosphite served as the reductant and source of phosphorus. The compositions of the bath are listed in Table 1. The total concentration of $NiSO_4{\cdot}6H_2O$ and $FeSO_4{\cdot}7H_2O$ was fixed at 22.5 g/L. The pH of the solution was adjusted to about 10 using $NH_3.H_2O$. The bath temperature was 70±1°C. Before deposition, each sample was pretreated with polishing and degreasing.

Table 1. Chemical components of Ni- Fe-P plating bath

Component	Concentration (g/L)
$(NH_4)_3C_6H_5O_7$	40
$FeSO_4{\cdot}7H_2O$	0-22.5
$NiSO_4{\cdot}6H_2O$	0-22.5
$NaH_2PO_2{\cdot}H_2O$	33
$C_{12}H_{12}O_{11}$	2
$NH_3.H_2O$	25 (mL/L)

The weight of Ni-Fe-P film was calculated by weighing the samples before and after deposition on copper foil(25×15×2 mm) by electronic microbalance model HT-300. The average plating rate was determined by dividing the film weight by the surface area of substrate and deposition time. The deposition time was recorded immediately after the sample immersing into the bath.

Polarization experiments were carried out in a three-compartment cell with the electrochemical analyzer CHI-660B. A platinum foil with size 20mm × 40mm was used as an auxiliary electrode and a saturated calomel electrode were used as reference electrode. The working electrode was the copper electrode (φ = 19 mm) embedded in an epoxy resin. In order to simulate partial cathodic or anodic reactions, the investigation of the electrolytes in the absence of either the $Na_2H_2PO_2$ reducer (oxidation solution) or the metal salts $FeSO_4$ and $NiSO_4$ (reducing solution) was also carried out.

The surface morphologies and compositions of the films were examined using scanning electron microscopy (SEM, JEOL JSM—6700) combined with energy dispersive spectrometry (EDS). The structure of the films was analyzed by XRD (Siemens D5000).

3. RESULTS AND DISCUSSION

In the initial stage of plating process, the plating rate was very slow due to the low activity of the copper sample. The reason is that copper is not a catalytic substrate for chemical deposition from hypophosphite solutions and the film growth starts at isolated locations on the substrate during chemical deposition[28-29]. As the discontinuous island structure grows into a continuous film, and the whole substrate is covered by lateral growth of Ni-Fe films, the autocatalytic activity of the sample increases, leading to the increase of plating rate. We refer the time required to form continuous film as the inducement time, which depends on the bath composition and plating conditions. To decrease the inducement time, the Ni-Fe-P deposition was initiated galvanically using aluminum at the beginning of the chemical process.

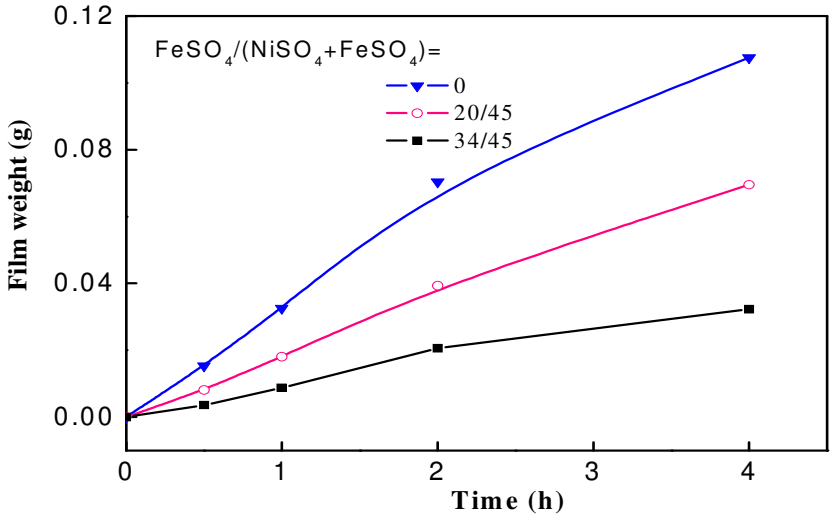

Figure 1. The plating rate dependence on plating time

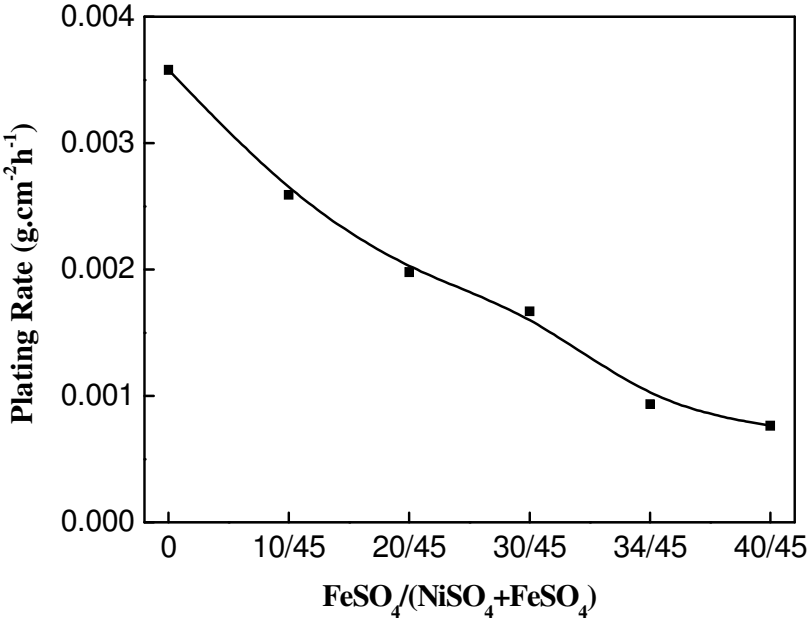

Figure 2. The plating rate dependence on ratio of $FeSO_4/(NiSO_4+FeSO_4)$

In order to elucidate the influence of the metal salt ratios (i.e., $FeSO_4/(NiSO_4+FeSO_4)$) on the Ni-Fe-P film, we begin with the study of the variations of the film weight and plating rate. Fig.1 depicts the dependence of the film weight on the plating time. It can be seen that the film weight increases near linearly with plating time, indicating that the plating rate keeps almost constant within the whole plating time. It is also obvious that the metal salt ratios dramatically affect the increasing rate of the film weight. The larger the ratio of $FeSO_4/(NiSO_4+FeSO_4)$, the more slowly the film weight increase with plating time, i.e., the plating rate of Ni-Fe-P films decreases with the increasing of $FeSO_4/(NiSO_4+FeSO_4)$ in the bath as shown in Fig.2. The small plating rate with higher $FeSO_4$ concentration is owing to the low catalytic activity and the inhibitory effect of iron on the chemical process, which is agreement with others' results [22,24,30]. Before the polarization measurement, the open-circuit potential both in reducing and oxidation solutions were recorded and listed in Table 2. The difference between the redox potential of the metal and that of the reductant, ΔE, is the force to drive deposition and related to the reaction rate. As shown in Table 2, the potential of copper electrode in oxidation solution is -1.024 V and those in reducing solution shifts negative, i.e., the drive force for the autocatalytic chemical deposition decreases with the $FeSO_4/(NiSO_4+FeSO_4)$ increasing.

Table 2. The open-circuit potential and polarization resistances in reducing and oxidation solutions

$FeSO_4/(NiSO_4+FeSO_4)$	1	40/45	30/45	20/45	10/45	0	oxidation solution
E_{open}	-1.012	-1.002	-0.984	-0.959	-0.946	-0.921	-1.024
*R*pc,*R*pa(Ω)	3.51	3.42	3.28	3.26	3.25	2.91	7.26

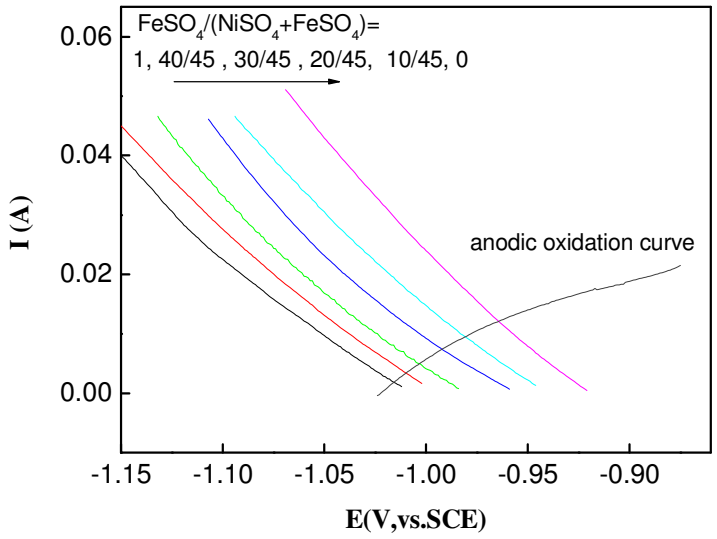

Figure 3. *I–E* partial curves for reduction of metal ions and for oxidation of hypophosphite

Fig.3 displays the anodic oxidation curve and the cathodic reducing curves with different ratios of $FeSO_4/(NiSO_4+FeSO_4)$. It can be seen that all the cathodic reducing curves intersect with the anodic oxidation curve. In terms of the mixed potential theory, the coordinates of the intersection of these polarization curves represent mixed potential (ordinate) and plating current (abscissa). The dependences of the mixed potential and plating current on the ratio of $FeSO_4/(NiSO_4+FeSO_4)$ are depicted in Fig.4. One can see that the mixed potential shifts negatively and plating current decreases with the increasing of ratio of $FeSO_4/(NiSO_4+FeSO_4)$. The negative potential shift with the increase of the ratio of FeSO4/(NiSO4+FeSO4) is caused by the change of solution chemistry. The cathodic and anodic resistances derived from the polarization curves are also presented in Table 2. The anodic resistance is more than twice of cathodic resistance, indicating the oxidation of $H_2PO_2^-$ controls the chemical process. The cathodic resistance increases and the plating rate decreases with the increasing of ratio of $FeSO_4/(NiSO_4+FeSO_4)$. This implies that the presence of ferrous sulfate in the baths had an inhibitory effect on the films deposition.

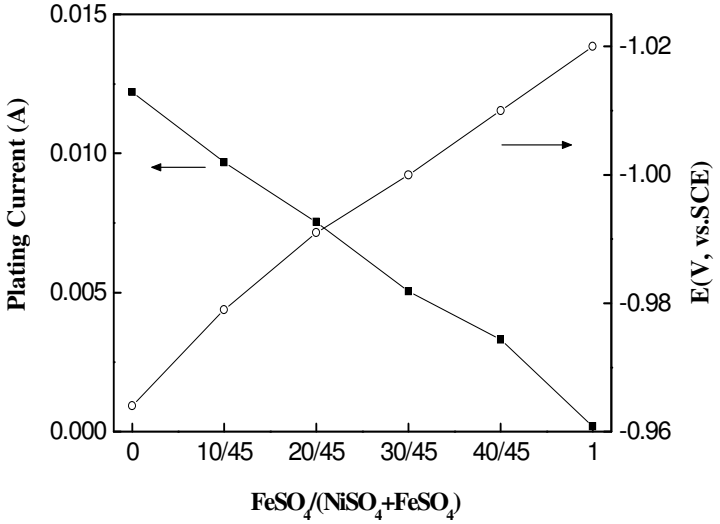

Figure 4. The dependences of the mixed potential and plating current on the ratios of $FeSO_4/(NiSO_4+FeSO_4)$ derived from partial polarization

Fig.5 illustrates the Tafel polarization curves, which were obtained by scanning the potential at a rate of 1 mV s^{-1} in the range ±150 mV of the open circuit potential E_{mix} in the Ni-Fe-P complete bath with different ratios of $FeSO_4/(NiSO_4+FeSO_4)$. The plating current was calculated using equation $i_d = \frac{K}{R_p}$, in which $K(=\frac{b_a b_c}{2.303(b_a + b_c)})$ is the polarization constant, R_p is the polarization resistance. The anodic b_a and cathodic b_c Tafel slopes were determined from these polarization curves. Compared with those derived from the polarization curves in Fe-B bath, the Tafel slopes are a little lower [27], the anodic Tafel slope b_a is about twice of cathodic Tafel slope b_c, which increases with the increasing of $FeSO_4/(NiSO_4+FeSO_4)$. The polarization resistance R_p was determined from the linear polarization experiments by scanning the potential ±15 mV about the open circuit potential at the same rate. The

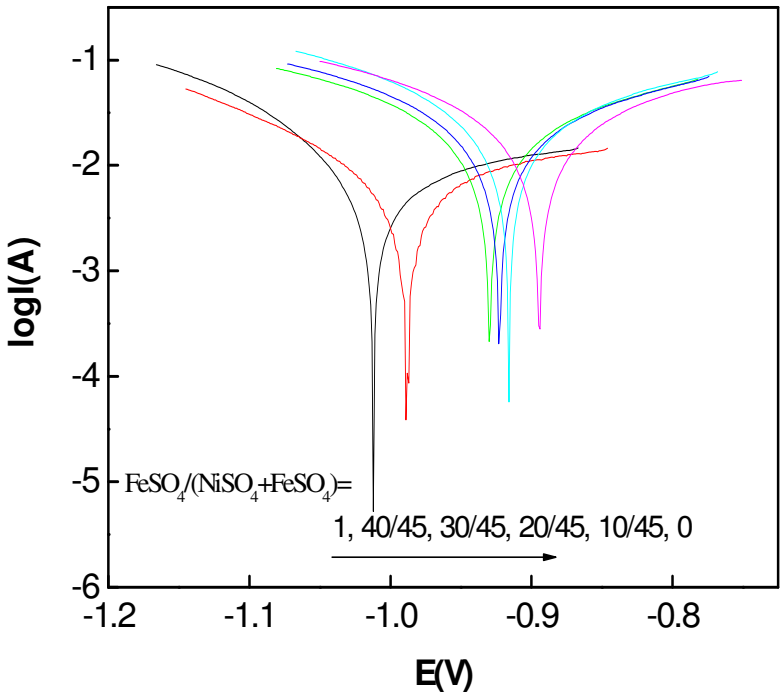

Figure 5. Tafel polarization curves in the electroless Fe-Ni-P complete bath

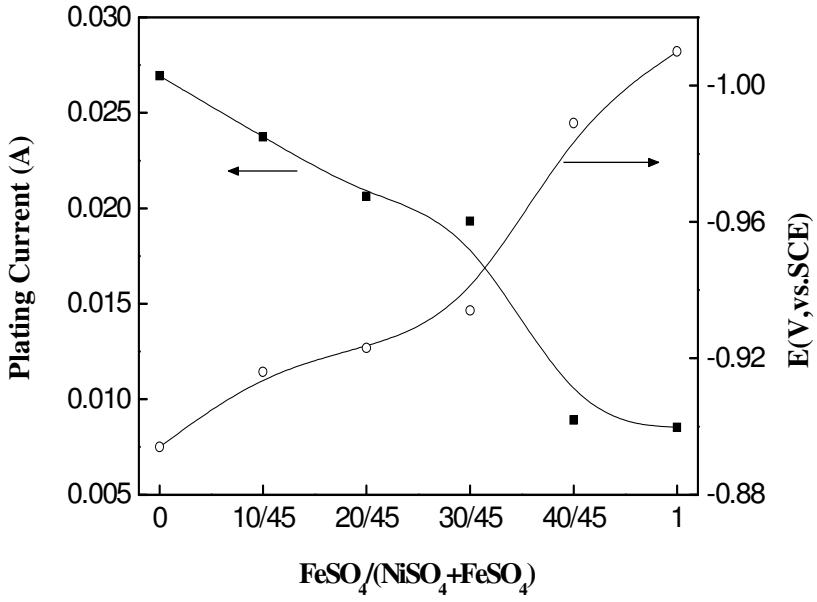

Figure 6. The dependences of plating current and potential on the ratios of $FeSO_4/(NiSO_4+FeSO_4)$ derived from Tafel polarization curves

mixed potential and plating current determined from these curves are presented in Fig.6. It can be seen that the dependences of the mixed potential and plating current on ratio of $FeSO_4/(NiSO_4+FeSO_4)$

show similar tendency to those derived from partial polarization curves as shown in Fig.4, i.e., the mixed potential shifts negatively and the plating current decreases with the ratio of $FeSO_4/(NiSO_4+FeSO_4)$ increasing. However, the mixed potential determined from the polarization in the complete bath is a little positive to that derived from the partial polarization curves, and plating current from the polarization in the complete bath is higher than that from the partial polarization curves. The possible reason for the magnitude difference between the plating current derived from the polarization curves in the complete bath and that in the simulation half-reaction cells is that the reduction of metal ions and the oxidation of hypophosphite is accelerated to some extent due to the interaction between the two half reactions on the catalytic surface. The plating rate, v_2(g/cm^2·h), can also be calculated from the plating current, i_{dep} (A/dm^2), using Faraday's law

$$v_2 = \frac{i_{dep}}{F}\frac{W}{n} = 0.373Ni_{dep} = 1.082\times10^{-2}\times i_{dep}(g\cdot cm^{-2}\cdot h^{-1})$$

where F is the Faraday constant, W the average atomic weight of film (supposing W= 58), n the number of electrons obtained by metal ion (n = 2), N=W/2 = 29. As shown in Fig.7, the plating rates derived from polarization curves show similar trend to that determined from weight method (Fig.2), i.e., the plating rates decrease with the increasing of $FeSO_4/(NiSO_4+FeSO_4)$. While the plating rates calculated from electrochemical measurement are significantly higher than the average plating rates determined from gravimetrical measurements. The possible reason for the magnitude difference between the plating rates is that the reduction of iron(nickel) ions and hypophosphite is suppressed to some extent due to hydrogen evolution , and/or the formation of the metal phosphides(hydroxide).

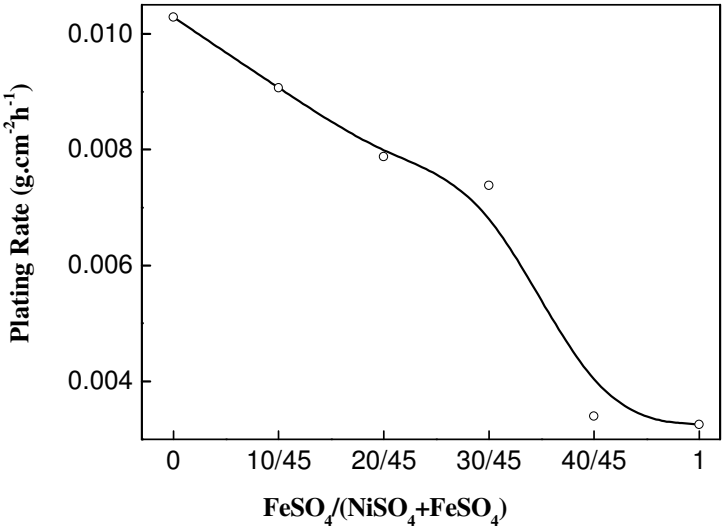

Figure 7. The plating rate dependence on ratio of $FeSO_4/(NiSO_4+FeSO_4)$ derived from polarization measurement

Now, we turn to study the influence of the metal salt ratios (i.e., $FeSO_4/(NiSO_4+FeSO_4)$) on the structure and composition of the Ni-Fe-P film. The XRD patterns of Ni-Fe-P films are displayed in Fig.8. It can be seen that the structure of the films depends on the ratio of $FeSO_4/(NiSO_4+FeSO_4)$. The films obtained in the bath with the ratios of $FeSO_4/(NiSO_4+FeSO_4)$ equal to 35/45 and 10/45 are in crystalline, while that equal to 30/45 shows typical amorphous diffraction patterns. This result is

Table 3. Chemical compositions of Ni- Fe-P films

$FeSO_4/(NiSO_4+FeSO$		35/45	30/45	10/45
Component Content (atom %)	P	21.27	26.12	21.84
	Fe	6.86	4.38	4.51
	Ni	71.87	69.50	73.65

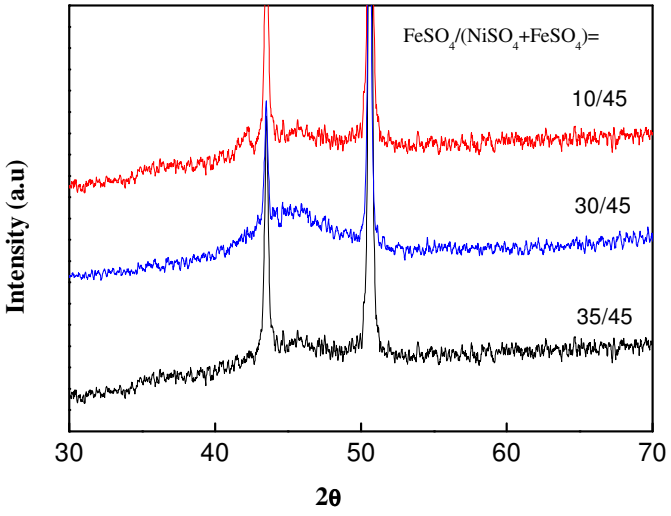

Figure 8. The XRD patterns of Ni–Fe–P alloys

similar to that observed in the Ref.18. The compositions of the Ni-Fe-P films determined by EDS are shown in Table 3. With the increase of the ratio of $FeSO_4/(NiSO_4+FeSO_4)$ in bath, nickel content in the film decreases, while iron content increases. When the ratio equals 30/45, the phosphorus content arrives at 26.12 atom%, leading to the amorphous nature of Ni-Fe-P film (as shown in Fig.8). According to electrochemical model, the electroless deposition can be divided into two processes: anodic and cathodic reactions. In the electroless bath with hypophosphite as the reductant, the anodic reaction is the oxidation of hypophosphite:

$$H_2PO_2^- + H_2O \rightarrow H_2PO_3^- + 2H^+ + 2e$$

At the same time, released electrons take part in the cathodic reactions. These reactions are reduction of nickel ions and hydrogen ions, accompanied with reduction of phosphorous and codeposition of iron. They can be presented as follows

$$Ni^{2+} + 2e \rightarrow Ni$$
$$2H^{+} + 2e \rightarrow H_2$$
$$H_2PO_2^{-} + 2H^{+} + e \rightarrow P + H_2O$$
$$Fe^{2+} + 2e \rightarrow Fe$$

The change of phosphorus content in the film is probably due to the oxidizing ability of hypophospite and the reducing ability of hypophosphite anion, which increases with the increase of Ni^{2+}. It is well known that in the absence of catalytic surfaces the hypophosphite species are quite stable and hypophosphite anion cannot be separately reduced in aqueous solution, by contrast they can be oxidized accompanied with phosphorous codeposition in the presence of certain metals such as nickel[31-33]. The electrons released by oxidation of hypophosphite are obtained by nickel ions, hydrogen ions, iron ions and hypophosphite anion competitively. When the concentration of the $NiSO_4$ is low, the oxidizing ability of hypophospite and the reducing ability of hypophosphite anion increase with the increasing of $NiSO_4$, leading to the increase of phosphorus content in the film. Further increasing the $NiSO_4$ increases the free Ni^{2+} in the bath, more electrons are captured by Ni^{2+}, nickel content increases while phosphorus content in the film decreases. Thus the change of composition and structure of the film may be attributed to the competitive reduction of several ions, such as nickel ions, hydrogen ions, iron ions, and hypophosphite anion.

4. CONCLUSIONS

The composition and structure of the Ni-Fe-P film can be controlled by the ratio of $FeSO_4/(NiSO_4+FeSO_4)$. When the ratio equals 30/45, the phosphorus content arrives at 26.12 atom%, leading to the amorphous nature of the film. Increasing the $FeSO_4$ concentration shifts the deposition potential positively and causes a decrease of the plating currents while an increase in the polarization resistances, indicating the $FeSO_4$ has an inhibition effect on the chemical process. The plating current derived in the complete bath is higher than that determined from the simulation half-reaction cells due to the interaction between the two half reactions.

ACKNOWLEDGEMENTS
This work was supported by Hunan Provincial Natural Science Foundation of China (Grant No. 05JJ30089).

References

1. M. Volmer and J. Neamtu, *Physica B: Condensed Matter*, 372 (2006)198
2. A. Sukiennicki, L. Wojtczak, I. Zasada and F.L. Castillo Alvarado, *Journal of Magnetism and Magnetic Materials*, 288 (2005) 137
3. S.F. Cheng, P. Lubitz, Y. Zheng and A.S. Edelstein, *Journal of Magnetism and Magnetic Materials*, 282 (2004) 109
4. P.L. Cavallotti, B. Bozzini, L. Nobili and G. Zangari, *Electrochimica Acta*, 39 (1994) 1123
5. P.M. Jacquart, L.Roux, *Journal of Magnetism and Magnetic Materials*, 281 (2004) 82
6. T. Osaka, *Electrochimica Acta*, 47 (2001) 23
7. T. Yokoshima, D. Kaneko, M. Akahori, H.S. Nam and Tetsuya Osaka, *Journal of Electroanalytical Chemistry*, 491 (2000) 197
8. M. Volmer and J. Neamtu, *Journal of Magnetism and Magnetic Materials*, 272-276 (2004) 1881
9. J.S. Chen, S.P. Lau, Y.B. Zhang, Z.Sun, B.K. Tay and C.Q. Sun, *Thin Solid Films*, 443 (2003) 115
10. N.V. Myung, D.Y. Park, B.Y. Yoo and P.T.A. Sumodjo, *Journal of Magnetism and Magnetic Materials*, 265 (2003) 189
11. J. Neamtu and M. Volmer, *Surface Science*, 482-485 (2001) 1010
12. U. Gradmann and H. J. Elmers, *Journal of Magnetism and Magnetic Materials*, 206 (1999) 107
13. A.F. Schmeckenbecher, *Journal of the Electrochemical Society*, 113 (1966) 778
14. W.O. Freitag, J.S. Mathas, G. DiGuilio, *Journal of the Electrochemical Society*, 111 (1964) 35
15. T. Osaka, *Electrochimica Acta*, 44 (1999) 3885
16. M. Sridharan, K. Shepoard, *Journal of Applied Electrochemistry*, 27 (1997) 1198
17. M. H. Seo, D. J. Kim, J. S. Kim, Thin Solid Films, 489(2005): 122
18. L.L. Wang, L.H. Zhao, G.F. Huang, *Surface and Coatings Technology*, 126 (2000) 272
19. G. Gabrielly, F. Raulin, *Journal of Applied Electrochemistry*, 1 (1971) 167
20. J. Kivel, J.S. Sallo, *Journal of the Electrochemical Society*, 112 (1965) 1201
21. L. Das, D.T. Chin, *Plating and Surface Finishing*, 83 (1996) 55
22. S.L. Wang, *Surface and Coatings Technology*, 186 (2004) 372
23. N.Petrov, Y.Sverdlov, Y. Shacham-Diamand, *Journal of the Electrochemical Society*, 149 (2002)C187
24. G.F Huang, W.Q Huang, L.L. Wang, Y. Meng, Z. Xie and B.S. Zou, *Electrochimica Acta*, 51 (2006) 4471
25. A.F. Schmeckenbecher, *Journal of the Electrochemical Society*, 113 (1966) 778
26. Y.S. Chang, I.J. Hsieh, *Plating and Surface Finishing*, 77 (1990) 52
27. G.F. Huang, W.Q. Huang, L.L. Wang, Y.C. Zhu, J.H Zhang, Q.L. Wang, *International Journal of Electrochemical Science*, 1 (2006) 354
28. H. Matsubara, T. Yonekawa, Y. Ishino, N. Saito, *Electrochimica Acta*, 52(2006): 402
29. R.C. Agarwala, V. Agarwala, *Sadhana*, 28, Parts 3&4 (2003) 475
30. W.Y. Hu, B.W. Zhang, *Physica B,* 175 (1991) 396
31. M.E.Touhami, E.Chassaing, M.Cherkaoui, *Electrochimica Acta*, 48 (2003) 3651
32. I.Ohno, O.Wakabayashi, S.Haruyama, *Journal of the Electrochemical Society*, 132 (1985) 2323
33. M. Saitou, Y.Okudaira, W.Oshikawa, *Journal of the Electrochemical Society*, 150 (2003) C140